Diamond & Related Materials 75 (2017) 44–51

Contents lists available at ScienceDirect

Diamond & Related Materials

journal homepage: www.elsevier.com/locate/diamond

# Nanocrystalline diamond films grown at very low substrate temperature using a distributed antenna array microwave process: Towards polymeric substrate coating

B. Baudrillart, F. Bénédic *, Th. Chauveau, A. Bartholomot, J. Achard

*LSPM-CNRS, UPR 3407, Université Paris 13, Sorbonne Paris Cité, 99 Avenue J. B. Clément, 93430 Villetaneuse, France*

ARTICLE INFO

*Article history:*
Received 21 November 2016
Received in revised form 29 December 2016
Accepted 1 January 2017
Available online 4 January 2017

*Keywords:*
Nanocrystalline
Diamond film
Plasma CVD
Surface characterization
Microstructure

ABSTRACT

The growth of NanoCrystalline Diamond (NCD) films at very low substrate temperature on large area surface using a distributed antenna array (DAA) microwave reactor operating in $H_2/CH_4/CO_2$ gas mixture is investigated. The estimated activation energy is in the range 1.3–3.2 kcal·mol$^{-1}$ depending on the injected microwave power and resulting substrate temperature range, which is comparable to values reported for other low-temperature NCD growth processes. The ability of the DAA reactor to deposit NCD films at a surface temperature down to 130 °C is demonstrated. NCD films composed of nanometric grains of 4.5 nm with a surface roughness of 27 nm are thus obtained, with a growth rate of 5 nm·h$^{-1}$. The decrease of the deposition temperature is followed by an increase of the renucleation rate leading to a reduction of the grain size and to a subsequent promotion of non-diamond phases. At this temperature, the decrease of the $CH_4$ percentage in the feed gas permits to improve the film purity but leads to a drastic decrease of the growth rate down to 2.5 nm·h$^{-1}$. Finally, a successful attempt of NCD film deposition on polytetrafluoroethylene (PTFE) substrate is shown aiming at exploring the coating of temperature-sensitive polymeric substrates employed for biomedical applications.



## 1. Introduction

Diamond is an excellent candidate for mechanical, optical, thermal, biomedical and electronic applications [1]. More specifically, Nanocrystalline Diamond (NCD) films have been the subject of an increasing interest for the last 20 years because of their very low thickness-dependent roughness and specific properties resulting from the nanometer-scale grain size and relatively large fraction of non-diamond phases localized at grain boundaries [2]. Combining suitable properties such as surface smoothness, high hardness, low friction coefficient and biocompatibility, NCD is one of the emerging materials for micro- and nano-electrical mechanical systems (MEMS, NEMS), surface acoustic wave (SAW) devices and biomedical applications [3]. For example, the implantation of NCD coated orthopedic screws into a human organism was successfully demonstrated without transplant rejection [4].

However, some of these applications require substrates that are temperature-sensitive with most of time a very low melting temperature. This is the case for polytetrafluoroethylene (PTFE), more and more used for biomedical applications such as bone regeneration or cardiovascular engineering [5,6], which has a melting point of 330 °C. Besides, combination of PTFE with Diamond-Like-Carbon (DLC) or NCD films showed an improvement of its functional properties, for example in the case of interactions with human osteoblastic cells [7,8]. Therefore, the development of new NCD synthesis processes operating at low deposition temperature is needed in order to avoid substrate damages and property modifications during growth. Furthermore, industrial scale applications necessitate deposition processes compatible with large area treatment.

Recently, in order to unlock technological obstacles and explore the coating of novel and innovative substrates, new deposition microwave reactors working at low temperature (typically lower than 500 °C) and on large area (from 20 × 20 to 30 × 30 cm$^2$) emerged, using $H_2/CH_4/CO_2$ gas mixture [9–12]. In the particular case of the high plasma density Distributed Antenna Array (DAA) reactor [13], low temperature NCD growth was demonstrated down to 250 °C on silicon and silicon nitride ($Si_3N_4$) substrates [14]. Thus, in order to allow the treatment of other temperature-sensitive substrates, the growth process using such a reactor has to be considered and optimized for deposition temperature lower than 250 °C.

In this paper, we investigate the aptitude of the DAA reactor for growing NCD films at very low substrate temperature down to 130 °C. Firstly, the effects of the deposition temperature on the characteristics of the films synthesized on silicon substrates, such as surface roughness, morphology, microstructure and growth rate, are assessed. Secondly,

* Corresponding author.
*E-mail address:* fabien.benedic@lspm.cnrs.fr (F. Bénédic).

http://dx.doi.org/10.1016/j.diamond.2017.01.001
0925-9635/

the influence of the gas mixture composition is examined at very low deposition temperature. Finally, a first attempt of NCD layer deposition on polytetrafluoroethylene (PTFE) substrate at 130 °C in optimized growth conditions is presented.

## 2. Experimental

Full description of the low temperature and large area deposition DAA reactor has already been given elsewhere [12]. Succinctly, the DAA reactor consists of 16 coaxial plasma sources arranged in 4 × 4 matrix fed by a 6 kW microwave generator working at 2.45 GHz. Discharges are ignited around each elementary source in $H_2/CH_4/CO_2$ feed gas and form uniform plasma which diffuses to the substrate. The temperature of the substrate is monitored by a thermocouple located in the 4-inch molybdenum substrate holder, very close to the backside of the substrate, and controlled with a graphite resistor through a PID regulator. For a good thickness homogeneity, *i.e.* deviation less than 10%, the distance between the elementary sources and the substrate is fixed at 95 mm. Polished (100) silicon wafers with thickness around 550 μm (n-type, 5–10 $\Omega \cdot cm^{-1}$, semiconductor grade) of 4-inch diameter are used as substrates. Prior to the growth step, the wafers were cleaned in acetone and rinsed in ethanol, and then seeded by spin coating with 25 nm nanodiamond particles in colloidal solution [15]. The standard growth conditions are characterized by a gas pressure of 0.35 mbar, a total gas flow rate of 50 sccm and a feed gas composition of 96.5%/2.5%/1% for $H_2/CH_4/CO_2$ precursors. These operating conditions allow the synthesis of diamond films down to 400 °C, with nanocrystalline features characterized by a surface morphology showing non-faceted particles with a grain size in the range 10–20 nm and a thickness-independent surface roughness typically around 10 nm [12]. For these reasons diamond films elaborated in the DAA system are designated as NCD films.

In the first part of this study we aim at investigating the ability of the DAA reactor for NCD film growth at very low surface temperature in the range 100–400 °C. In absence of a cooling system the only way to significantly decrease the substrate temperature is to turn off the heating system and to decrease the injected microwave power. A surface temperature between 130 and 300 °C can be then reached when the heating system is off for a microwave power varying between 1.2 and 3 kW. The microwave power and the resulting substrate temperature for samples achieved as a function of the deposition temperature in standard conditions are reported in Table 1 (samples A–D). For each microwave power employed, the effect of a variation of the substrate temperature in a range 300–400 °C on the growth rate is also investigated by switching on the additional heating system and varying the current intensity passing through the graphite resistor.

In the second part of the paper, the effects of the $CH_4$ concentration decrease are investigated at 130 °C in order to improve NCD film quality. In comparison with sample D, the $CH_4$ percentage was fixed to 1.5 and 1% for samples E and F, respectively (Table 1).

Finally, in the last part the NCD growth on polytetrafluoroethylene (PTFE) polymeric temperature-sensitive substrates, prepared by using the *ex situ* pretreatment described above, excepted acetone rinsing, is examined at 130 °C in the growth conditions of sample D (Table 1, sample G).

**Table 1**
Sample deposition conditions.

| Sample name | Substrate | Power [kW] | Temperature [°C] | $H_2$ [%] | $CH_4$ [%] | $CO_2$ [%] |
|---|---|---|---|---|---|---|
| A | Silicon | 3 | 400 | 96.5 | 2.5 | 1 |
| B | | 3 | 300 | | | |
| C | | 2 | 230 | | | |
| D | | 1.2 | 130 | | | |
| E | Silicon | 1.2 | 130 | 97.5 | 1.5 | 1 |
| F | | 1.2 | 130 | 98 | 1 | 1 |
| G | PTFE | 1.2 | 130 | 96.5 | 2.5 | 1 |

The deposition duration was set between 4 and 23 h, depending on growth conditions, in order to obtain continuous films with thicknesses around 100 nm.

The film morphology was investigated by top-view Scanning Electron Microscopy (SEM) images taken by a field emission ZEISS ULTRA plus SEM system. Surface roughness was measured with a VEECO Dimension 3100 Atomic Force Microscopy (AFM) system in tapping mode in air.

The Raman spectra were obtained with a HR800 (HORIBA Jobyn-Yvon) working in a confocal mode and in the back-scattering configuration, using a continuous-wave diode-pumped solid state laser (CoboltblueTM) at 473 nm as an excitation source with a power of 50 mW. The quality of the deposited films may be roughly estimated from deconvoluted Raman spectra through the $sp^3$ fraction defined as:

$$sp^3(\%) = 100 \cdot \left( \frac{60 \cdot I_{\text{diamond}}}{60 \cdot I_{\text{diamond}} + \sum I_{\text{non diamond}}} \right) \quad (1)$$

where $I_{\text{diamond}}$ is the Raman diamond peak area at 1332 $cm^{-1}$, which represents $sp^3$ phase, and $\sum I_{\text{non diamond}}$ is the sum of Raman non diamond peak areas. A Raman signal efficiency factor averaged ratio of 60 between non diamond and $sp^3$ phases, mainly weighted by the response of the graphite G band centered at 1580 $cm^{-1}$, was used for the considered excitation wavelength.

X-Ray Diffraction (XRD) patterns were obtained using $CuK_{\alpha 1}$ radiation ($\lambda = 1.54056$ Å) with an incident angle of 1°. The grain size was estimated using modified Scherrer equation applied on the (111) and (220) diamond diffraction peaks [16]. Film thickness was measured by three methods: *(i)* UV–visible reflectometer (NanoCalc, Ocean Optics), *(ii) in situ* visible interferometry, and *(iii)* weight gain measurement after growth.

## 3. Results and discussion

Previous plasma investigations have pointed out a limited dependency of some process key-species densities such as $CH_3$, $C_2H_2$, CO and H, measured at the substrate position as a function of the injected microwave power in the range 2–3 kW [17]. In the same time, the gas temperature measured through $H_2$ molecule emission significantly decreases from 700 to 400 °C when the microwave power decreases from 3 to 1 kW [18]. The diminishing of the gas temperature thus leads to a significant reduction of the substrate temperature without requiring additional cooling system so that 130 °C can be reached for 1.2 kW.

For the three microwave powers reported in Table 1, *i.e.* 1.2, 2 and 3 kW, the effects of the substrate temperature were first investigated on the growth rate in order to allow comparisons of the process activation energy according to the following Arrhenius equation:

$$G = G_0 \exp(-E_a/RT) \quad (2)$$

where $G$ is the growth rate, $G_0$ is a temperature-independent constant, $E_a$ is the activation energy, $R$ is the universal gas constant ($1.989\ cal \cdot K^{-1} \cdot mol^{-1}$) and $T$ is the substrate temperature.

The Arrhenius diagram of the growth rate estimated for the films grown at 1.2, 2 and 3 kW for a temperature range of 130–400 °C, 230–600 °C and 300–600 °C, respectively, are given in Fig. 1. According to Eq. (2), the activation energy derived from the gradient of a least-square fitting of the growth rate values are $E_a^{1.2\ kW} = 1.3 \pm 0.2\ kcal \cdot mol^{-1}$, $E_a^{2\text{-}kW} = 1.46 \pm 0.15\ kcal \cdot mol^{-1}$ and $E_a^{3\ kW} = 3.2 \pm 0.2\ kcal \cdot mol^{-1}$.

It should be reminded here that a single activation energy should be ideally related to a one-step reaction leading to the growth process and characterized by a single activation barrier. For the considered experimental conditions, no thorough reaction scheme describing all NCD

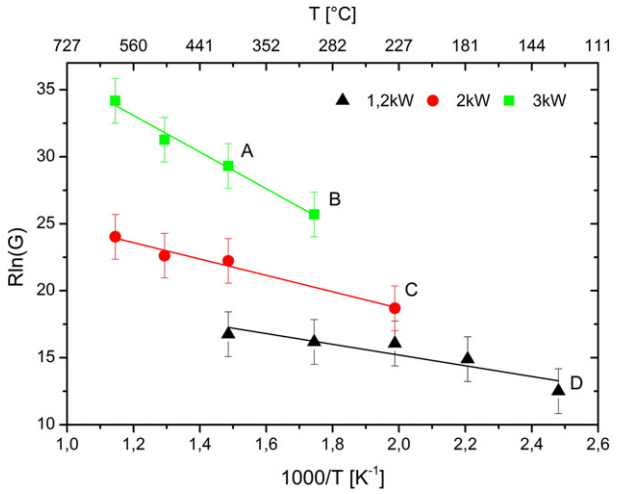


**Fig. 1.** Arrhenius plot of NCD film growth rate at 3, 2, 1.2 kW for the corresponding temperature ranges of 300–600 °C, 230–600 °C and 130–400 °C, respectively. The conditions of samples A, B, C and D are shown.

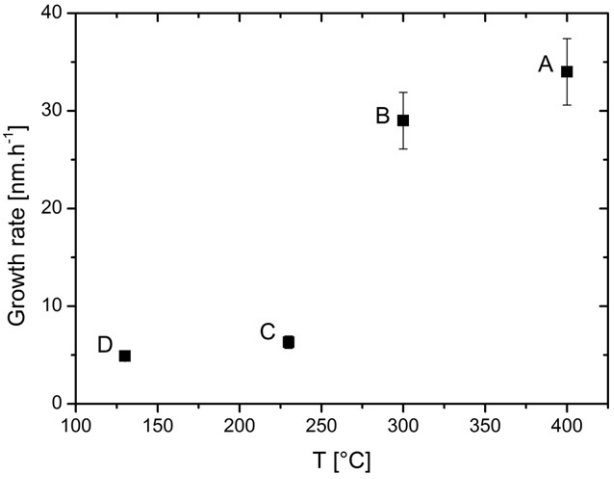


**Fig. 2.** Growth rate measured for NCD films grown on samples A, B, C and D at 400, 300, 230 and 130 °C, respectively.

growth mechanisms that may be involved by using $H_2/CH_4/CO_2$ feed gas has been yet reported. Consequently, it is not possible to highlight a possible dominant reaction which would be characterized by a single activation energy. Therefore, the activation energy considered here is related to the whole growth process including various mechanisms such as species addition and abstraction at the surface sites, dehydrogenation of adsorbed carbon containing radicals, *etc*. The activation energy discussed hereafter may be understood as an *apparent* activation energy that permits to compare different growth conditions and different growth processes in term of efficiency.

For high temperature range between 500 and 900 °C commonly used for NCD growth by microwave plasma enhanced CVD process using $Ar/H_2/CH_4$ or $H_2/CH_4$ gas mixtures, the reported activation energy is in the range 6–9 kcal·mol$^{-1}$ [19–21]. For the highest microwave power considered here and a substrate temperature between 300 and 600 °C, the activation energy is 3.2 kcal·mol$^{-1}$, which is lower by a factor two. For close temperature range, the activation energy determined here for 2 kW microwave power is significantly lower with a value of 1.46 kcal·mol$^{-1}$. This underlines the possible influence of the species temperature on the growth rate, but also the probable contribution of growth and etching species, the density of which may depends on the microwave power. Also the effectiveness of gas precursor fragmentation should be considered. In previous work [17], higher fragmentation efficiency for $CH_4$, $CO_2$ and also $H_2$ was found at 2 kW compared to 3 kW, which means that more precursors are dissociated by energy unit.

The activation energy value of 1.3 kcal·mol$^{-1}$ measured here for the lower microwave power and the subsequent temperature range of 130–400 °C is slightly lower than that reported in other works for low temperature NCD synthesis microwave processes using $H_2/CH_4/CO_2$ gas mixture estimated between 1.6 and 2 kcal·mol$^{-1}$ [22,23]. In general case, a lower activation energy may be due to a higher defect density promoted by a higher renucleation rate [24]. Therefore, the particular design of the DAA reactor is suitable for improving the deposition process efficiency at low surface temperature.

The growth rate of samples B, C and D measured for the lower deposition temperature of 300, 230, 130 °C, allowed by the corresponding microwave power of 3, 2 and 1.2 kW, respectively, is shown Fig. 2. Sample A, which was deposited at 400 °C and 3 kW is considered as a reference sample. For samples A and B, the growth rate perceptively decreases from 34 to 29 nm·h$^{-1}$, which is only due to the change of the deposition temperature. Between samples B and C a wide gap of the growth rate is noticed with values of 29 nm·h$^{-1}$ and 6.5 nm·h$^{-1}$, respectively. For sample D achieved at 130 °C, a growth rate of 5 nm·h$^{-1}$ is found. The decrease trend can be linked to surface phenomena occurring during the growth. Indeed, physical and chemical reactions during diamond deposition are temperature dependent, in particular the sticking coefficients of growth species, such as methyl radical, on diamond surface. A decay of the sticking coefficients of $CH_3$ with the gas temperature has thus been reported when considering diamond synthesis using $H_2/CH_4$ conventional process [25]. The fraction of dangling bonds on the surface, acting as growth sites during the deposition process, may also be influenced by the surface temperature. An estimation of the dependency of the dangling bond fraction as a function of substrate temperature and $[H]/[H_2]$ ratio was proposed by May et al. [26]. This fraction decreases with the temperature. Both phenomena could lead to the decrease of the growth rate with substrate temperature and microwave power.

The top view micrographs of samples A-D are reported in Fig. 3. For all the samples, the film morphology is characterized by a granular surface where no emerging well-facetted crystallites can be observed. This is typical of NCD films obtained on silicon substrates at low pressure and low temperature in DAA reactor, which are formed of ball-shape aggregates [15].

The surface topography of the samples is presented in Fig. 4 through the AFM micrographs of the films. For sample A, C and D an average value of 150 nm in size is found for the aggregates, whereas a slightly larger size of 250 nm is measured for sample B. However, the surface root mean square roughness (Rms) monotonically raises from 11 to 27 nm while the surface temperature diminishes from 400 to 130 °C.

Raman spectra of the considered samples are shown in Fig. 5. For all the samples, the diamond peak at 1332 cm$^{-1}$ is well visible along with the broad bands centered at 1350 cm$^{-1}$ and 1580 cm$^{-1}$, which correspond to graphite D and G bands, respectively. The finger print of nanocrystalline diamond through the trans-polyacetylene responses at around 1140 cm$^{-1}$ and 1480 cm$^{-1}$ is also noticed [27,28]. The spectra exhibit a drastic decrease of the diamond peak intensity and a noticeable raise of the graphite bands when the surface temperature is decreased. The $sp^3$ fraction estimated from Eq. (1) thus evolves from 80 to 55%. These trends can be related to the grain size diminishing, which increases the proportion of grain boundaries that are mainly composed of non-diamond phases [24]. This is consistent with the increase of the full width at half maximum (FWHM) of the 1332 cm$^{-1}$ diamond peak as shown in the inset of Fig. 5, which is due to a decrease of the grain size and raise of the degree of structural disorder in the diamond crystallites [29].

Four distinct diffraction peaks relative to silicon substrate and diamond film can be seen on XRD patterns reported in Fig. 6. The most important contribution is due to the (311) diffraction peak of silicon substrate at $2\theta = 56.1°$. The three other diffraction peaks clearly visible

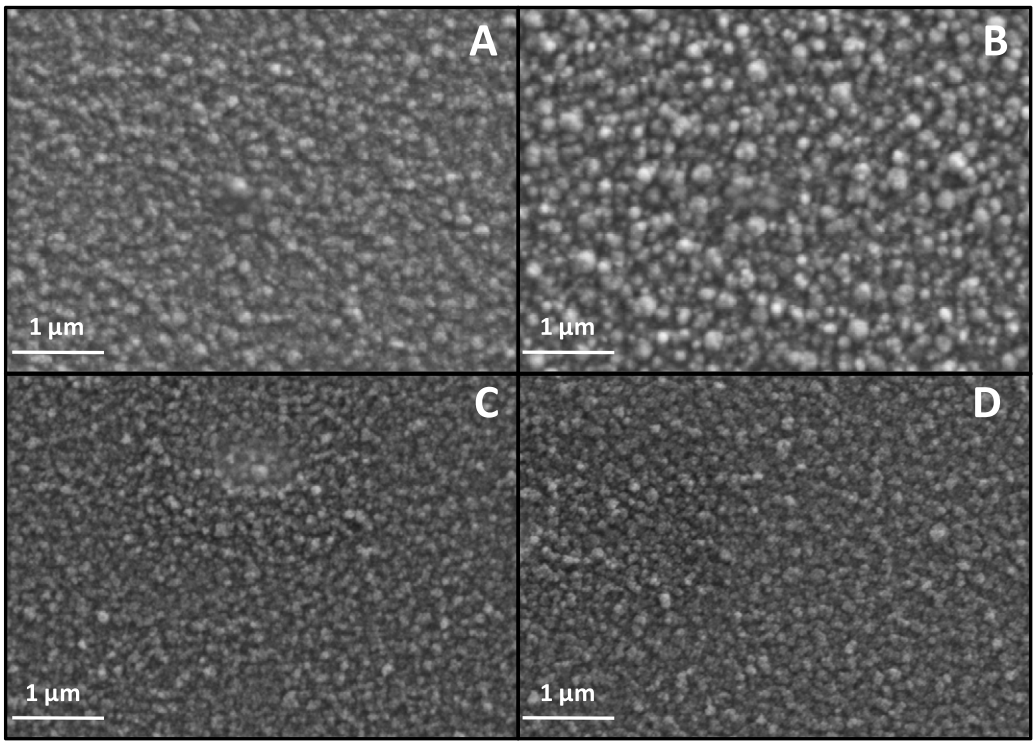


**Fig. 3.** SEM micrographs of samples A, B, C and D grown at 400, 300, 230 and 130 °C, respectively.

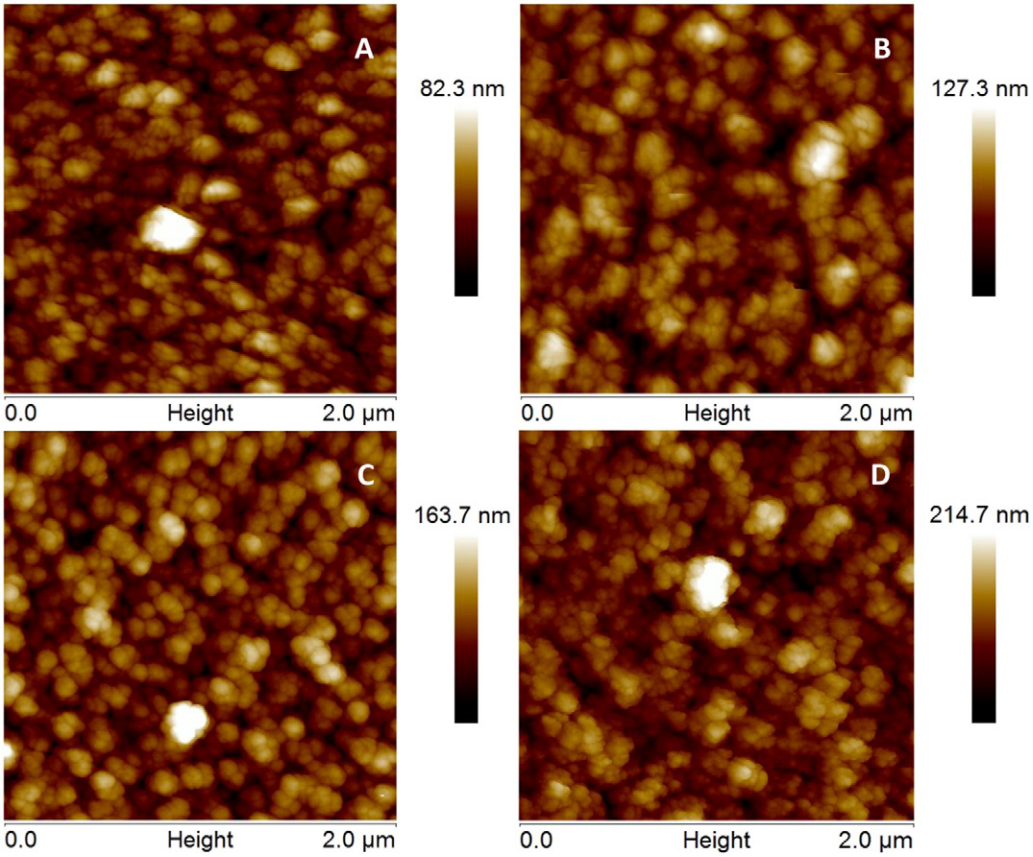


**Fig. 4.** AFM micrographs of samples A, B, C and D grown at 400, 300, 230 and 130 °C, respectively.

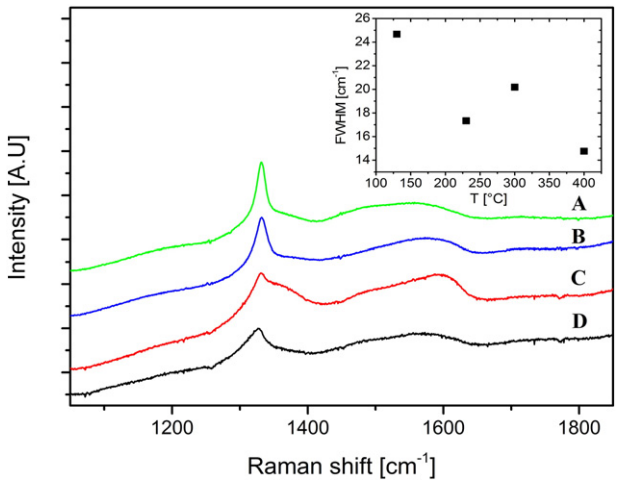


**Fig. 5.** Raman spectra of samples A, B, C and D grown at 400, 300, 230 and 130 °C, respectively. The inset figure shows the FWHM of the diamond peak at 1332 $cm^{-1}$ as a function of the growth temperature.

for samples A-C at $2\theta = 43.9°$, 75.3° and 91.5° are relative to the (111), (220) and (311) crystalline plans of cubic diamond, respectively. Sample D only exhibits small diamond (111) and (220) diffraction peaks. Furthermore, slight broad contributions, especially for $2\theta$ in the range 80°–95°, are observed for the four samples, particularly for sample D, which could be diffuse background related to amorphous components [29].

The modified Scherrer equation applied on the (111) and (220) diamond diffraction peaks allowed us to calculate the Diffracting Coherent Domain (DCD) size, which can be considered to be representative of the grain size, taking into account the line relative intensity, width, and relative position. The strong decrease of the grain size with the substrate temperature is assessed in Fig. 7. The grain size is around 20 nm at 400 °C and drastically diminishes by a factor 4 down to 4.5 nm at 130 °C. This is in good agreement with the qualitative trend described for the FWHM of diamond peaks in Raman spectra. The decrease of the grain size with the deposition temperature is also consistent with the evolution of diamond and graphite peak intensities described for Raman spectra, since the proportion of grain boundaries containing non-diamond phases is promoted.

Fig. 7 also shows the evolution of surface Rms roughness as a function of the substrate temperature. A surprising opposite trend with respect to grain size is observed with a raise by more than factor 2 from 11 to 27 nm while the substrate temperature decreases from 400 °C to

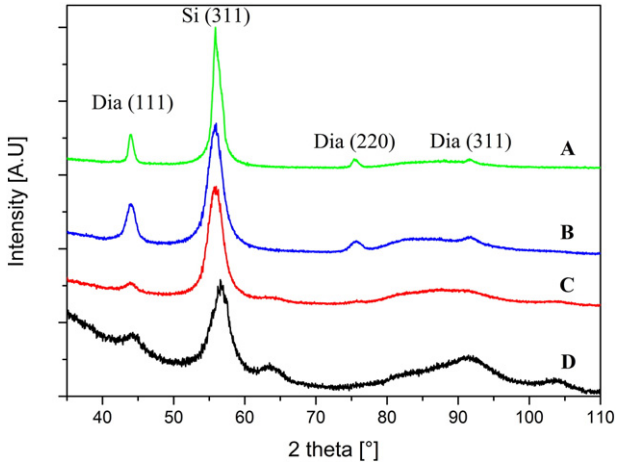


**Fig. 6.** XRD patterns of sample A, B, C and D grown at 400, 300, 230 and 130 °C, respectively.

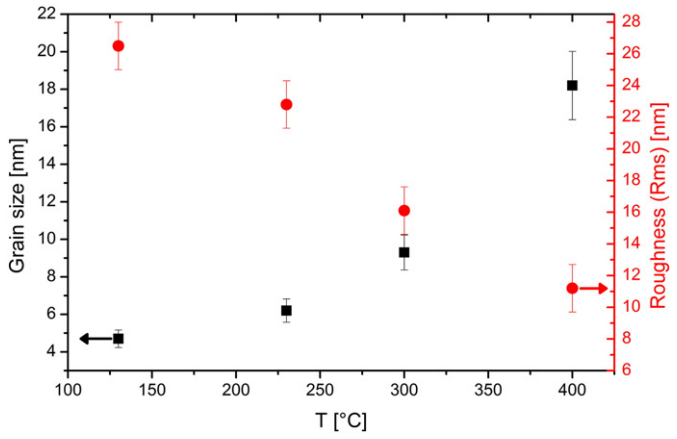


**Fig. 7.** Size of DCD and surface Rms roughness for samples A, B, C and D grown at 400, 300, 230 and 130 °C, respectively.

130 °C. It should be recalled here that the low temperature NCD films achieved in the DAA reactor are formed of aggregates composed of nanocrystalline diamond grains [14,15,21]. Hence the surface roughness is mainly governed by the aggregate shape and size instead of the nanocrystalline diamond grain size. The decrease of the grain size with the deposition temperature results from the increase of the renucleation rate as discussed before, which may promote a higher defect density. These defects act as nucleation sites for the growth of new nanocrystalline diamond grains but also new aggregates. Thus, for a high renucleation rate, *i.e.* at very low substrate temperature and low microwave power, the initiation of the next layer growth could proceed before all the voids in the current layer are filled [30]. This may lead to an increase of the film porosity and of the surface topography, even for comparable aggregate size, as observed through the Rms roughness behavior as a function of the substrate temperature (Fig. 7).

In this first part, the ability of the DAA reactor to deposit NCD films at very low surface temperature down to 130 °C has been demonstrated and discussed. However, the decrease of the deposition temperature is followed by an increase of the renucleation rate leading to a reduction of the grain size and to a subsequent promotion of non-diamond phases. The renucleation rate could be reduced by restraining the amount of $CH_4$ in the gas phase [30]. Thus, in the following part, the effects of the decrease of $CH_4$ percentage in the feed gas from 2.5 to 1% at 130 °C is investigated through sample D as reference and samples E and F (Table 1).

The surface morphology observed by SEM for sample D, E and F is presented in Fig. 8. The films are continuous and its aspect is comparable with aggregates covering the whole surface. Nevertheless, the films become denser as the $CH_4$ concentration in the feed gas diminishes with less and less void between the aggregates. As described previously the formation of such diamond layers with decreasing porosity results from a decrease of the renucleation rate.

The decrease of the film porosity is followed by a decay of the surface Rms roughness from 27 to 12 nm as shown in Fig. 9. In the same time, the grain size estimated from DCD size assessed by XRD increases from 4.5 to 9 nm. The same opposite trend as a function of $CH_4$ concentration than the one discussed when varying the substrate temperature (Fig. 7) is thus observed for the grain size and surface topography. As expected, the decrease of $CH_4$ concentration induces the raise of the grain size, as reported in other works [31], because of a lower renucleation rate. The correlated lower defect density leads then to a better arrangement of the aggregates and consequently to a decrease of the surface roughness. This behavior should be understood as a consequence of a dual growth/renuclation process during the NCD films synthesis [30].

Limitation of the contribution of non-diamond phase containing grain boundaries and/or increase of diamond proportion, as the grain size evolves with $CH_4$ concentration decay, can be directly linked to the $sp^3$ fraction estimated from Eq. (1), which increases from 55 to

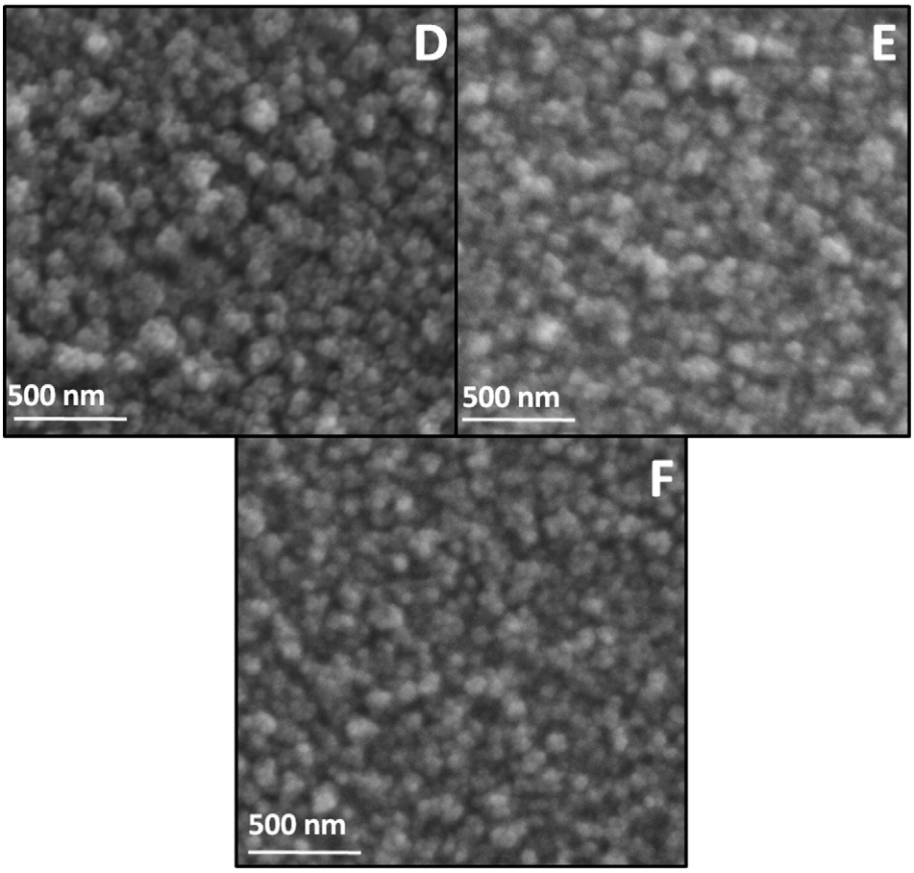


**Fig. 8.** SEM micrographs of sample D, E and F grown at 130 °C with 2.5, 1.5 and 1% $CH_4$ in the gas mixture, respectively.

almost 90% (Fig. 10). In terms of plasma composition, the diminution of the $CH_4$ percentage causes both a decrease of carbon containing precursors and an increase of $H_2$ and $CO_2$ in the feed gas. These species would be dissociated in H-atoms and other oxygen containing species that could improve the stabilization of the growing diamond surface and the etching of non-diamond phases [32–35]. The enhancement of both coupled phenomena leads to a decrease of the growth rate with $CH_4$ amount by a factor 2, from 5 to 2.5 $nm \cdot h^{-1}$, as emphasized in Fig. 10.

The decrease of the $CH_4$ percentage permits to improve the NCD film quality but provokes a dramatic decay of the growth rate. Therefore, the best compromise between a satisfactory quality and an acceptable growth rate for NCD film deposition at surface temperature as low as 130 °C corresponds to the synthesis conditions of sample D. For these reasons, the possibility of NCD deposition on polymeric PTFE substrate has been investigated in these latter conditions.

Raman characterization was performed on the PTFE substrate before and after growth in order to distinguish the different Raman contributions, including diamond, non-diamond, but also PTFE responses, after diamond deposition process (Fig. 11). Raman spectrum of PTFE bare substrate exhibits three distinct peaks in the considered Raman shift range appearing at 1216, 1300 and 1381 $cm^{-1}$ as reported elsewhere [36]. The Raman spectrum after growth reveals an intense diamond peak at 1332 $cm^{-1}$ which establishes the successful diamond

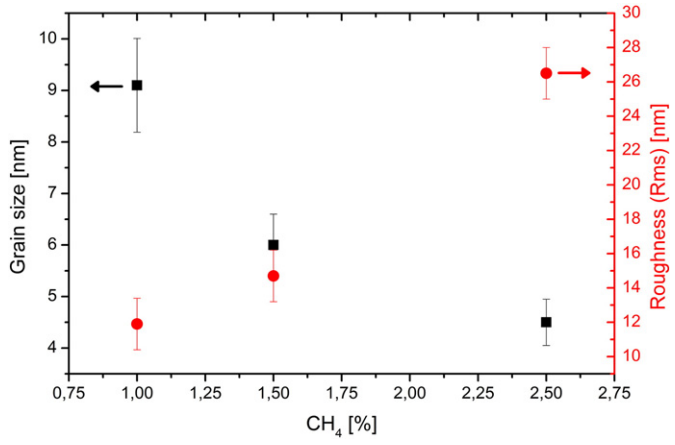


**Fig. 9.** Size of DCD and surface Rms roughness for samples D, E and F grown at 130 °C with 2.5, 1.5 and 1% $CH_4$ in the gas mixture, respectively.

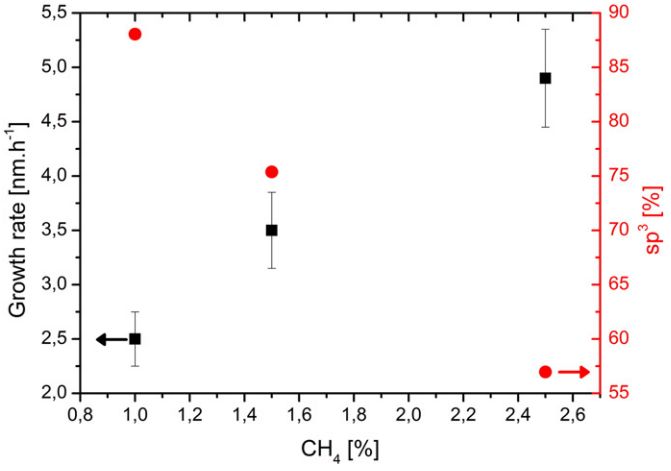


**Fig. 10.** Growth rate and $sp^3$ fraction estimated from Raman spectra for samples D, E and F grown at 130 °C with 2.5, 1.5 and 1% $CH_4$ in the gas mixture, respectively.

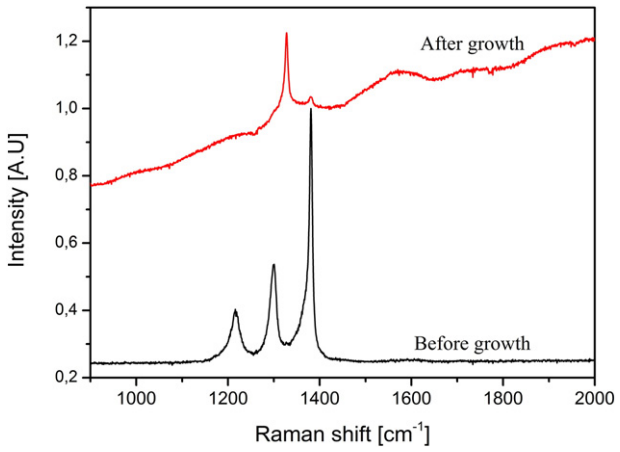


**Fig. 11.** Raman spectra of sample G (PTFE substrate) before and after deposition in the DAA reactor at 130 °C.

deposition. The PTFE contribution through its three characteristic peaks is still present, particularly the most intense line at 1381 $cm^{-1}$. The broad band between 1070 and 1250 $cm^{-1}$ is due to the convolution between the 1140 $cm^{-1}$ trans-polyacetylene band and the 1216 $cm^{-1}$ PTFE peak, which is a sign of the film nanocrystalline diamond feature. Finally, the base of the diamond peak is slightly enlarged due to the convolution with the 1300 $cm^{-1}$ PTFE peak. These observations point out the growth of NCD film on PTFE substrate in the DAA reactor at 130 °C. However, adhesion of NCD films on this kind of polymeric substrate is poor and requires optimization through further investigations especially concerning the *ex situ* pretreatment.

## 4. Conclusion

In this paper we investigated the DAA reactor capability to grow NCD diamond films at very low substrate temperature, down to 130 °C, using $H_2/CH_4/CO_2$ gas mixture at 0.35 mbar.

The deposition temperature was controlled by adjusting an additional substrate heating system and the injected microwave power. A deposition temperature of 400, 300, 230 and 130 °C can be then reached for a microwave power in the range 1.2–3 kW. All the conditions considered here were suitable for the growth of diamond films with nanocrystalline structure.

The activation energy was first investigated for a microwave power of 1.2, 2 and 3 kW. It was estimated at 1.3 kcal·$mol^{-1}$ at 1.2 kW and the subsequent substrate temperature between 130 and 400 °C. This value is slightly lower than those reported in literature for comparable temperature range. This low activation energy could be due to the coupled effects of a higher renucleation rate and a higher gas precursor fragmentation efficiency yielded in the DAA reactor.

The decrease of the deposition temperature from 400 to 130 °C leads to a significant change of the film microstructure. At very low substrate temperature the measured grain size is 4.5 nm but the surface roughness is increased up to 27 nm due to the raise of the renucleation rate and of the resulting film porosity with respect to ball-shape aggregate arrangement. Also the non-diamond phases are promoted as an effect of the increase of the grain boundary proportion, so that $sp^3$ fraction decreases from 80 to 55%. The growth rate decreases from 34 to 5 nm·$h^{-1}$, which has been discussed in term of surface phenomena including sticking coefficient and dangling bond fraction.

At 130 °C, the decrease of the $CH_4$ percentage in the feed gas, from 2.5 to 1%, permits to improve the film purity because of the decrease of the renucleation rate conducting to an increase of the grain size limiting the grain boundaries and non-diamond phase amount. The $sp^3$ fraction thus evolves from 55 to 90%. This is accompanied by a drastic decrease of the growth rate down to 2.5 nm·$h^{-1}$ which prohibits the use of such films for most of potential industrial applications.

Finally, a successful attempt of NCD growth on PTFE substrate in the DAA reactor at 130 °C was demonstrated.

The ability to control the grain size and film porosity at very low deposition temperature by varying the process parameters will be investigated in forthcoming works in order to control and improve some film properties such as topography, friction coefficient or thermal conductivity.

## References

[1] B. Dischler, C. Wild, Low -Pressure Synthetic Diamond: manufacturing and Applications, Springer Series in Materials Processing, Springer, 1998.
[2] D.M. Gruen, Nanocrystalline diamond films 1, Annu. Rev. Mater. Sci. 29 (1999) 211–259.
[3] O.A. Williams, Nanodiamond, RSC Nanoscience & Nanotechnology 31 (2014) (Cambridge).
[4] S.F. Mitura, K. Mitura, P. Niedzielski, P. Louda, V.V. Danilenko, Nanocrystalline diamond, its synthesis, properties and applications, Journal of Achievements in Materials and Manufacturing Engineering 16 (2006) 9–16.
[5] W. Becker, C. Dahlin, B.E. Becker, U. Lekholm, D. Van Steenberghe, K. Higuchi, C. Kultje, The use of e-PTFE barrier membranes for bone promotion around titanium implants placed into extraction sockets: a prospective multicenter study, Int. J. Oral Maxillofac. Implants 9 (1994) 31–40.
[6] B. Yashiro, M. Shoda, Y. Tomizawa, T. Manaka, N. Hagiwara, Long-term results of a cardiovascular implantable electronic device wrapped with an expanded polytetrafluoroethylene sheet, J. Artif. Organs 15 (2012) 244–249.
[7] L. Bacakova, L. Grausova, J. Vacik, A. Fraczek, S. Blazewicz, A. Kromka, M. Vanecek, V. Svorcik, Improved adhesion and growth of human osteoblast-like MG 63 cells on biomaterials modified with carbon nanoparticles, Diam. Relat. Mater. 16 (2007) 2133–2140.
[8] A. Calzado-Martín, L. Saldaña, H. Korhonen, A. Soininen, T.J. Kinnari, E. Gómez-Barrena, V.-M. Tiainen, R. Lappalainen, L. Munuera, Y.T. Konttinen, Interactions of human bone cells with diamond-like carbon polymer hybrid coatings, Acta Biomater. 6 (2010) 3325–3338.
[9] J. Kim, K. Tsugawa, M. Ishihara, Y. Koga, M. Hasegawa, Large-area surface wave plasmas using microwave multi-slot antennas for nanocrystalline diamond film deposition, Plasma Sources Sci. Technol. 19 (2010) 015003.
[10] K. Tsugawa, M. Ishihara, J. Kim, M. Hasegawa, Y. Koga, Large-area and low-temperature nanodiamond coating by microwave plasma chemical vapor deposition, New Diamond and Frontier Carbon Technology 16 (2006) 347-346.
[11] A. Kromka, O. Babchenko, T. Izak, K. Hruska, B. Rezek, Linear antenna microwave plasma CVD deposition of diamond films over large areas, Vacuum 86 (2012) 776–779.
[12] H.A. Mehedi, J. Achard, D. Rats, O. Brinza, A. Tallaire, V. Mille, F. Silva, C. Provent, A. Gicquel, Low temperature and large area deposition of nanocrystalline diamond films with distributed antenna array microwave-plasma reactor, Diam. Relat. Mater. 47 (2014) 58–65.
[13] L. Latrasse, A. Lacoste, J. Sirou, J. Pelletier, High density distributed microwave plasma sources in a matrix configuration: concept, design and performance, Plasma Sources Sci. Technol. 16 (2007) 7–12.
[14] B. Baudrillart, F. Bénédic, A.S. Melouani, F.J. Oliveira, R.F. Silva, J. Achard, Low-temperature deposition of nanocrystalline diamond films on silicon nitride substrates using distributed antenna array PECVD system, Phys. Status Solidi A 213 ( 2016) 2575–2581.
[15] B. Baudrillart, F. Bénédic, O. Brinza, T. Bieber, T. Chauveau, J. Achard, A. Gicquel, Microstructure and growth kinetics of nanocrystalline diamond films deposited in large area/low temperature distributed antenna array microwave-plasma reactor, Phys. Status Solidi A 212 (2015) 2611–2615.
[16] H.M. Rietveld, Line profiles of neutron powder-diffraction peaks for structure refinement, Acta Crystallogr. 22 (1967) 151.
[17] A.S.C. Nave, B. Baudrillart, S. Hamann, F. Bénédic, G. Lombardi, A. Gicquel, J.H. van Helden, J. Röpcke, Spectroscopic study of low pressure, low temperature $H_2$–$CH_4$–$CO_2$ microwave plasmas used for large area deposition of nanocrystalline diamond films. Part II: on plasma chemical processes, Plasma Sources Sci. Technol. 25 (2016) 065003.
[18] A.S.C. Nave, B. Baudrillart, S. Hamann, F. Bénédic, G. Lombardi, A. Gicquel, J.H. van Helden, J. Röpcke, Spectroscopic study of low pressure, low temperature $H_2$–$CH_4$–$CO_2$ microwave plasmas used for large area deposition of nanocrystalline diamond films. Part I: on temperature determination and energetic aspects, Plasma Sources Sci. Technol. 25 (2016) 065002.
[19] T.G. McCauley, D.M. Gruen, A.R. Krauss, Temperature dependence of the growth rate for nanocrystalline diamond films deposited from an Ar/$CH_4$ microwave plasma, Appl. Phys. Lett. 73 (1998) 1646–1648.
[20] T. Izak, O. Babchenko, S. Potocky, Z. Remes, H. Kozak, E. Verveniotis, B. Rezek, A. Kromka, Low temperature diamond growth, RSC Nanoscience & Nanotechnology 31 (2014) 290–342 Chapter 13.
[21] B. Baudrillart, A.S.C. Nave, S. Hamann, F. Bénédic, G. Lombardi, J.H.V. Helden, J. Röpcke, J. Achard, Growth processes of nanocrystalline diamond films in microwave cavity and distributed antenna array systems: a comparative study, Diam. Relat. Mater. 71 (2017) 53–62.

[22] K. Tsugawa, M. Ishihara, J. Kim, Y. Koga, M. Hasegawa, Nanocrystalline diamond film growth on plastic substrates at temperatures below 100 °C from low-temperature plasma, Phys. Rev. B 82 (2010).
[23] T. Izak, O. Babchenko, M. Varga, S. Potocky, A. Kromka, Low temperature diamond growth by linear antenna plasma CVD over large area, Phys. Status Solidi B 249 (2012) 2600–2603.
[24] D.C. Barbosa, P.R.P. Barreto, V.W. Ribas, V.J. Trava-Airoldi, E.J. Corat, Diamond nanostructures growth, Encyclopedia of Nanoscience and Nanotechnology 10 (2009) 3–10.
[25] L. Schwaederlé, P. Brault, C. Rond, A. Gicquel, Molecular dynamics calculations of $CH_3$ sticking coefficient onto diamond surfaces, Plasma Process. Polym. 12 (2015) 764–770.
[26] P.W. May, Y.A. Mankelevich, From ultrananocrystalline diamond to single crystal diamond growth in hot filament and microwave plasma-enhanced CVD reactors: a unified model for growth rates and grain sizes, J. Phys. Chem. C 112 (2008) 12432–12441.
[27] A.C. Ferrari, J. Robertson, Origin of the 1150 $cm^{-1}$ Raman mode in nanocrystalline diamond, Phys. Rev. B 63 (2001).
[28] R. Pfeiffer, H. Kuzmany, P. Knoll, S. Bokova, N. Salk, B. Günther, Evidence for trans-polyacetylene in nano-crystalline diamond films, Diam. Relat. Mater. 12 (2003) 268–271.
[29] L. Fayette, B. Marcus, M. Mermoux, G. Tourillon, K. Laffon, P. Parent, F. Le Normand, Local order in CVD diamond films: comparative Raman, x-ray-diffraction, and x-ray-absorption near-edge studies, Phys. Rev. B 57 (1998) 14123.
[30] P.W. May, M.N.R. Ashfold, Y.A. Mankelevich, Microcrystalline, nanocrystalline, and ultrananocrystalline diamond chemical vapor deposition: experiment and modeling of the factors controlling growth rate, nucleation, and crystal size, J. Appl. Phys. 101 (2007) 053115.
[31] O.A. Williams, A. Kriele, J. Hees, M. Wolfer, W. Müller-Sebert, C.E. Nebel, High Young's modulus in ultra thin nanocrystalline diamond, Chem. Phys. Lett. 495 (2010) 84–89.
[32] J.C. Angus, C.C. Hayman, Low-pressure, metastable growth of diamond and "diamondlike" phases, Science 241 (1988) 913–921.
[33] M. Ihara, H. Maeno, K. Miyamoto, H. Komiyama, Low-temperature deposition of diamond in a temperature range from 70 °C to 700 °C, Diam. Relat. Mater. (1992) 187–190.
[34] A. Vescan, W. Ebert, T.H. Borst, E. Kohn, Electrical characterisation of diamond resistors etched by RIE, Diam. Relat. Mater. 5 (1996) 747–751.
[35] J. Stiegler, T. Lang, M. Nygard-Ferguson, Y. von Kaenel, E. Blank, Low temperature limits of diamond film growth by microwave plasmaassisted CVD, Diam. Relat. Mater. 5 (1996) 226–230.
[36] A. Gruger, A. Régis, T. Schmatko, P. Colomban, Nanostructure of Nafion® membranes at different states of hydration: an IR and Raman study, Vib. Spectrosc. 26 (2001) 215–225.